reverse, TGGGTCGAAATCGTCCTCTTCTCAT; for *Pd-otx*: forward, ACTTGCCAGAAT CCAGAGTTCAGG; reverse, GGGACCATATTGAGGGCGAGTT; for *Pd-gsc*: forward, TGAACCAAACCTCAACCCTCTCTTCCT; reverse, GGACGATCTTTACGGATGAGCAA CTGG) and plasmid specific primers (T7 and T3) at 30 s 94 °C, 1 min 60 °C and 4 min 72 °C. We confirmed identity of the clones by sequencing (EMBL Nucleotide Sequence Database accession numbers: *Pd-bra*, PDU289022; *Pd-otx*, AJ278856; and Pd-*gsc*, PDU289023).

Phylogenetic analysis

We obtained protein sequences of a selected number of species from the database and aligned them using CLUSTALW. We used these alignments to calculate a phylogenetic tree using the maximum likelihood program PUZZLE[29].

Whole-mount *in situ* analysis

We fixed embryos in 4% paraformaldehyde /2 × PBS-Tween for 1–4 h. An established *in situ* hybrization protocol[30] was followed with the modification of Proteinase K treatment in 100 µg ml⁻¹ for 4 min (24 h larvae), or 10 min (72 h young worms). After staining, embryos were refixed in paraformaldehyde /2 × PBS-Tween, washed and cleared in 80% glycerol. We mounted embryos in glycerol and took pictures under Nomarsky optics using a Zeiss Axiophot.

1. Willmer, P. *Invertebrate Relationships* (Cambridge Univ. Press, Cambridge, 1990).
2. Nielsen, C. *Animal Evolution: Interrelationships of the Living Phyla* (Oxford Univ. Press, Oxford, 1995).
3. Grobben, K. Die systematische Einteilung des Tierreichs. *Verh. Zool. Bot. Ges. Wien* **58**, 491–511 (1908).
4. Dorresteijn, A. W. C., O'Grady, B., Fischer, A., Porchet-Henere, E. & Boilly-Marer, Y. Molecular specification of cell lines in the embryo of *Platynereis* (Annelida). *Roux's Arch. Dev. Biol.* **202**, 264–273 (1993).
5. Shoguchi, E., Satoh, N. & Maruyama, Y. K. Pattern of Brachyury gene expression in starfish embryos resembles that of hemichordate embryos but not sea urchin embryos. *Mech. Dev.* **82**, 185–189 (1999).
6. Peterson, K. J., Cameron, R. A., Tagawa, K., Satoh, N. & Davidson, E. H. A comparative molecular approach to mesodermal patterning in basal deuterostomes: the expression pattern of *Brachyury* in the enteropneust hemichordate *Ptychodera flava*. *Development* **126**, 85–95 (1999).
7. Tagawa, K., Humphreys, T. & Satoh, N. Novel pattern of *Brachyury* gene expression in hemichordate embryos. *Mech. Dev.* **75**, 139–143 (1998).
8. Shoguchi, E., Harada, Y., Numakunai, T. & Satoh, N. Expression of the Otx gene in the ciliary bands during sea cucumber embryogenesis. *Genesis* **27**, 58–63 (2000).
9. Harada, Y. *et al.* Developmental expression of the hemichordate *otx* ortholog. *Mech. Dev.* **91**, 337–339 (2000).
10. Steinbeisser, H. & De Robertis, E. M. *Xenopus goosecoid*: a gene expressed in the prechordal plate that has dorsalizing activity. *C. R. Acad. Sci.* **316**, 959–971 (1993).
11. Kispert, A., Herrmann, B. G., Leptin, M. & Reuter, R. Homologs of the mouse *Brachyury* gene are involved in the specification of posterior terminal structures in *Drosophila*, *Tribolium*, and *Locusta*. *Genes Dev.* **8**, 2137–2150 (1994).
12. Woollard, A. & Hodgkin, J. The *Caenorhabditis elegans* fate-determining gene mab-9 encodes a T-box protein required to pattern the posterior hindgut. *Genes Dev.* **14**, 596–603 (2000).
13. Kispert, A. & Herrmann, B. G. The *Brachyury* gene encodes a novel DNA binding protein. *EMBO J.* **12**, 3211–3220 (1993).
14. Peterson, K. J., Cameron, R. A. & Davidson, E. H. Bilaterian origins: significance of new experimental observations. *Dev. Biol.* **219**, 1–17 (2000).
15. Kusch, T. & Reuter, R. Functions for *Drosophila brachyenteron* and *forkhead* in mesoderm specification and cell signalling. *Development* **126**, 3991–4003 (1999).
16. Smith, J. *Brachyury* and the T-box genes. *Curr. Opin. Genet. Dev.* **7**, 474–480 (1997).
17. Wilson, E. B. The cell-lineage of *Nereis*. A contribution to the cytogeny of the annelid body. *J. Morphol.* **6**, 361–480 (1892).
18. Wu, L. H. & Lengyel, J. A. Role of caudal in hindgut specification and gastrulation suggests homology between *Drosophila* amnioproctodeal invagination and vertebrate blastopore. *Development* **125**, 2433–2442 (1998).
19. De Robertis, E. M. & Sasai, Y. A common plan for dorsoventral patterning in Bilateria. *Nature* **380**, 37–40 (1996).
20. Arendt, D. & Nübler-Jung, K. Dorsal or ventral: similarities in fate maps and gastrulation patterns in annelids, arthropods and chordates. *Mech. Dev.* **61**, 7–21 (1997).
21. Hirth, F. & Reichert, H. Conserved genetic programs in insect and mammalian brain development. *BioEssays* **21**, 677–684 (1999).
22. Hahn, M. & Jäckle, H. *Drosophila goosecoid* participates in neural development but not in body axis formation. *EMBO J.* **15**, 3077–3084 (1996).
23. Goriely, A. *et al.* A functional homologue of *goosecoid* in *Drosophila*. *Development* **122**, 1641–1650 (1996).
24. Yasuo, H. & Satoh, N. Conservation of the developmental role of *Brachyury* in notochord formation in a urochordate, the ascidian *Halocynthia roretzi*. *Dev. Biol.* **200**, 158–170 (1998).
25. Holland, P. W., Koschorz, B., Holland, L. Z. & Herrmann, B. G. Conservation of Brachyury (T) genes in amphioxus and vertebrates: developmental and evolutionary implications. *Development* **121**, 4283–4291 (1995).
26. Haeckel, E. in *Systematische Phylogenie. 2.Teil: Systematische Phylogenie der wirbellosen Thiere (Invertebrata).* 259–347 (Georg Reimer, Berlin, 1896).
27. De Robertis, E. M. Evolutionary biology. The ancestry of segmentation. *Nature* **387**, 25–26 (1997).
28. Arendt, D. & Nübler-Jung, K. Comparison of early nerve cord development in insects and vertebrates. *Development* **126**, 2309–2325 (1999).
29. Strimmer, K. & Von Haeseler, A. Likelihood-mapping: A simple method to visualize phylogenetic content of a sequence alignment. *Proc. Natl Acad. Sci. USA* **94**, 6815–6819 (1997).
30. Loosli, F., Köster, R. W., Carl, M., Krone, A. & Wittbrodt, J. Six3, a medaka homologue of the

Drosophila homeobox gene sine oculis is expressed in the anterior embryonic shield and the developing eye. *Mech. Dev.* **74**, 159–164 (1998).

Self-motion and the perception of stationary objects

Mark Wexler, Francesco Panerai, Ivan Lamouret & Jacques Droulez

Laboratoire de Physiologie de la Perception et de l'Action, Collège de France, 11 place Marcelin Berthelot, 75005 Paris, France

One of the ways that we perceive shape is through seeing motion[1–3]. Visual motion may be actively generated (for example, in locomotion), or passively observed. In the study of the perception of three-dimensional structure from motion, the non-moving, passive observer in an environment of moving rigid objects has been used as a substitute[1] for an active observer moving in an environment of stationary objects; this 'rigidity hypothesis' has played a central role in computational and experimental studies of structure from motion[4,5]. Here we show that this is not an adequate substitution because active and passive observers can perceive three-dimensional structure differently, despite experiencing the same visual stimulus: active observers' perception of three-dimensional structure depends on extraretinal information about their own movements. The visual system thus treats objects that are stationary (in an allocentric, earth-fixed reference frame) differently from objects that are merely rigid. These results show that action makes an important contribution to depth perception, and argue for a revision of the rigidity hypothesis to incorporate the special case of stationary objects.

The original work comparing actively produced to passively observed motion parallax[6,7] found structure from motion (SFM) performance that depended on retinal information alone: non-moving observers receiving optical information similar to that received by active observers had similar response thresholds. Other studies have found that self-motion helps to resolve discrete symmetries in optic flow[8,9], or to decrease integration times in SFM[10].

In the first experiment we tested extraretinal contributions to the extraction of depth from motion by means of a cue–conflict paradigm, in which motion parallax cues to three-dimensional (3D) structure were weighed against conflicting linear perspective (that is, the assumption that lines nearly parallel or perpendicular in the image are actually parallel or perpendicular in 3D space). The observer saw a planar 3D grid in motion, and estimated its tilt (the direction of its projected normal in the frontoparallel plane). Motion parallax could be actively produced or passively observed. In the active case, parallax was due to the observer's head movements around a virtual object; in the passive case, the observer remained still while watching a replay of the optic flow from a preceding active trial. The tilt of the plane defined by perspective

cues differed from the tilt defined by motion cues by $\Delta T = 0°$, 45°, 90°, 135° or 180°. further details and examples of stimuli are shown in Fig. 1.

In their tilt judgements, subjects could ignore one cue, switch between cues, or base their responses on a weighted average of the two cues—although theoretical considerations suggest that for large conflicts such as ours, cue averaging would not be optimal[11].

If on a particular trial the observer relied on the motion cue alone, he or she would perceive a spatially irregular structure that contradicted laws of linear perspective[12], but one that underwent rigid 3D motion. If the observer relied on the perspective cue alone, he or she would perceive a structure that was more spatially regular, but that underwent deformation in time, thus violating the rigidity assumption that is supposed to underlie SFM[5,13,14] (but see also
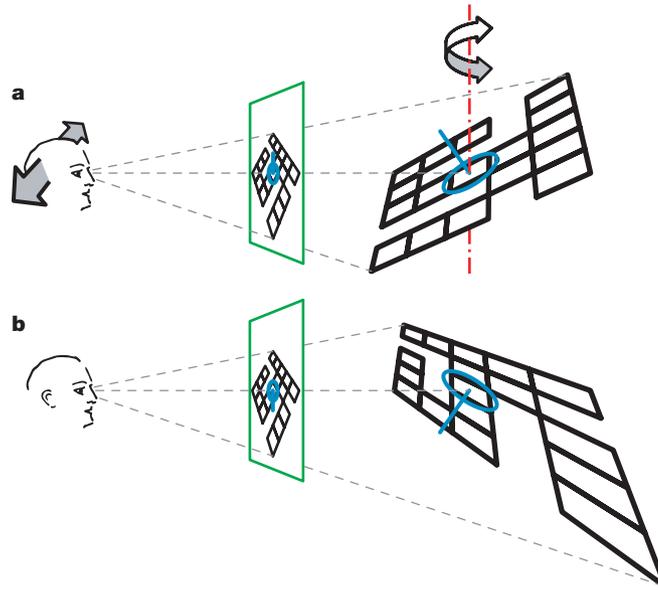

Figure 1 Stimuli used in the experiments. **a**, A no-conflict stimulus, where both perspective and motion cues indicate a surface tilted upwards. Motion was due either to subject's head movements, or to object rotation. Both the virtual object and its projection are shown. The subject's task was to line up a probe (shown in blue) with the surface. **b**, A conflict stimulus, generated by back-projecting the no-conflict stimulus onto a different plane. Although the virtual object is now tilted downwards, in its central position the projection is identical to the no-conflict stimulus; thus, perspective cues indicate upward tilt, while motion cues indicate downward tilt. In this case, the tilt conflict ΔT would be 180°.
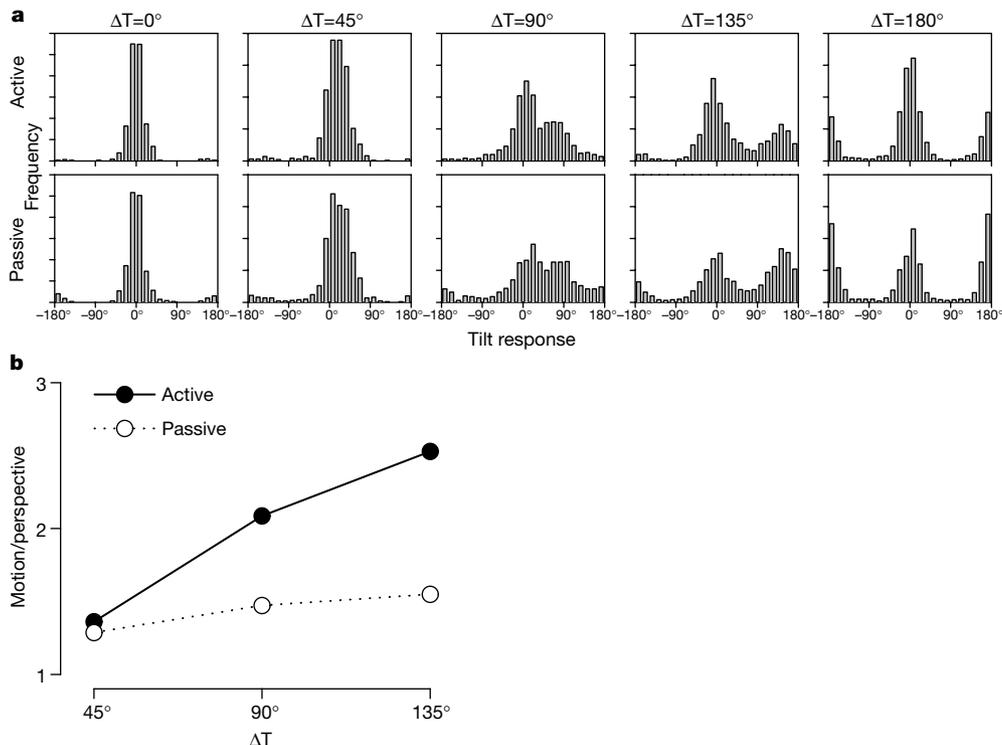
Figure 2 Results of experiment 1, averaged over subjects. **a**, Frequencies of tilt responses, in the active and passive conditions, for no tilt conflict ($\Delta T = 0°$) and tilt conflicts $\Delta T = 45°$, 90°, 135° and 180°. Responses are adjusted so that motion tilt is always at 0°, and so that perspective tilt is positive. **b**, The ratio of motion- to perspective-based responses in the active and passive conditions, as a function of tilt conflict.

refs 15–18)—as in the well-known Ames window phenomenon[19–23].

Tilt responses in experiment 1 are shown in Fig. 2a. If the response is in accordance with motion cues, we would expect a peak at 0° (all angles are defined with respect to motion tilt); if the response is in accordance with perspective cues, the peak would be at ΔT. Furthermore, motion cues can yield an 'inverted' response at $\pm 180°$, owing to the approximate symmetry of optic flow under the simultaneous inversion of motion and tilt; this symmetry is exact in the case of parallel projection but, in our case, the inverted solution is not perfectly rigid[8,9]. As can be seen from Fig. 2a, the responses are based on a multimodal mixture of perspective and motion cues (the multimodality is present in individual subject data), and, as predicted for large conflicts[11], not on cue averages.

The main effect of self-motion is on the relative strength of the motion and perspective cues: responses in accordance with motion cues are more frequent in the active than in the passive condition. In order to quantify this self-motion effect, we counted trials with responses based on motion cues, and those with responses based on perspective cues (see Fig. 2b). Motion responses are defined as those falling within $\pm 22.5°$ bins of 0° and 180°, perspective responses as those around ΔT. (Conditions $\Delta T = 0°$ and 180°, where there is a partial confound between the two types of responses, are excluded.) A three-way analysis of variance on ΔT, cue and self-motion variables showed a significant cue × self-motion interaction ($F_{1,7} = 6.53$, $P < 0.05$). A similar effect of self-motion was predicted[24] in discussing the Ames window (see ref. 25 for related work).

The other effect of self-motion is fewer inverted responses in the active condition: for $0° \leq \Delta T \leq 135°$, tilt responses in 7.1% of the trials are inverted (that is, they cluster around $T = 180°$) in the active condition, whereas 20.3% are inverted in the passive condition ($F_{1,7} = 25.4$, $P < 0.01$)[8,9]. On the other hand, the precision of tilt judgements was no different in the active than in the passive case. This can be shown by fitting the distributions in Fig. 2a with sums of gaussians centred about $T = 0$ and $T = \Delta T$. Mean widths of the $T = 0$ peaks were 27.3° and 27.1° for the active and passive cases, respectively, with the difference not significant. The similar precision of SFM in active and passive conditions echoes previous results[6,9], which also found that perception of 3D structure was not more precise in active than in passive observers.

A crucial difference between what subjects perceive in the active and passive conditions are spatial attributes of the object in an allocentric reference frame. When the observer utilizes motion depth cues at the expense of conflicting perspective, he or she perceives a rigid 3D object. In the active case, this rigid object is also stationary in an allocentric, earth-fixed reference frame, whereas in the passive case, the object specified by motion cues is no less rigid but undergoes movement in space[26,27]. In principle, stationarity—as opposed to rigidity—is impossible to reliably determine from optic information alone. (Physiologically, the visual system may sometimes be fooled into judging an object to be stationary from large-angle optic flow, as in the case of vection.) We propose that motion cues are enhanced in the active condition over the passive condition because in the former case they lead to percepts that are not only rigid, but also stationary: the 'stationarity hypothesis'. The relative dearth of inverted—and therefore non-stationary—solutions in active trials in experiment 1 is further, indirect evidence for the stationarity hypothesis. On the other hand, motion cues could simply be enhanced for an observer in motion. There is no way to distinguish the stationarity and the 'motion-enhancement' hypotheses in experiment 1, where moving observers always perceive stationary objects from motion cues.

We directly tested the stationarity hypothesis in a second experiment, which used the same active/passive cue–conflict paradigm as experiment 1. But here, on some active trials ('twist' trials), the virtual object was not stationary but underwent oscillations about a horizontal axis. In the absence of cue conflict, in the twist trials active observers correctly perceived an object undergoing rigid oscillatory motion, in synchrony with their own head movements. The stationarity hypothesis predicts that in active, non-stationary trials the use of motion cues would be reduced relative to active, stationary trials. On the other hand, if the enhancement of motion cues in the active condition of experiment 1 were due to mere presence of self-motion, we would expect no effect of non-stationarity.

As can be seen from Fig. 3a, responses on no-twist trials are similar to those in experiment 1. In twist trials without cue conflict, there is still a sharp peak about $\Delta T = 0$, showing that subjects were able to do the task even in the presence of a non-stationary stimulus synchronized with their own motion. In twist trials with cue conflict, on the other hand, the dominance of motion cues seen in the stationary case disappears, as predicted by the stationarity hypothesis, and is replaced by approximately equal peaks around motion and perspective cues, reminiscent of the passive condition in experiment 1. To quantify this result, we have counted motion- and perspective-based trials, as in experiment 1; their ratios are shown in Fig. 3b. The effect of stationarity on the active case was significant: in the $\Delta T = 90°$ case, there was an interaction between cue and twist variables ($F_{1,7} = 44.0$, $P < 0.001$). This effect is not due simply to the change in the axis of rotation that is introduced by the twist, as seen from a cue × twist × self-motion interaction ($F_{1,7} = 18.0$, $P < 0.01$). As predicted by the stationarity hypothesis, the highest ratio was in the one case (active, no-twist) where motion cues yielded a spatially stationary object.

In two experiments we show two results. The more general result
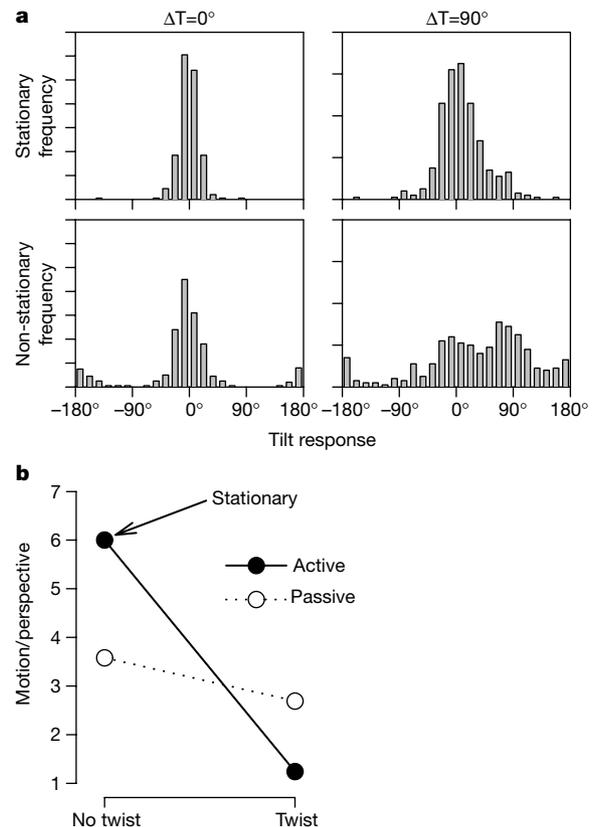

Figure 3 Results of experiment 2, averaged over subjects. **a**, Frequencies of tilt errors in active stationary and active non-stationary conditions, with and without tilt conflict. Passive results were similar to those in experiment 1, showing no effect of twist. **b**, Ratio of motion- to perspective-based responses with and without twist in active and passive conditions, with tilt conflict. Responses are defined as motion-based when tilt falls within $\pm 45°$ bins about 0° and 180° and as perspective-based when tilt falls within $\pm 45°$ of 90°.

is that extraretinal, self-motion information is incorporated into visual judgements of three-dimensional structure. The visual stimulation in the active and passive conditions of experiment 1 is the same, yet the active observer responds more frequently on the basis of motion cues than does the passive observer. Thus the effect of self-motion on spatial vision does not reduce to its modification of optic flow. The second result builds on the first: the relative enhancement of motion cues only occurs when they indicate objects that are stationary in an allocentric reference frame. It seems that the visual system is biased towards perceiving stationary objects, even when their image deforms as a result of observer motion. Physiological findings point to the existence of allocentric coding in mammalian brains[28] that could be involved in this process. Our results would point to a revision of the rigidity concept in SFM, and, more generally, the inadequacy of excluding observer motion in the analysis of spatial vision. □

Methods

Experiments were performed in monocular conditions in darkness. Translations of the subject's dominant eye were measured by a head tracker[29], sampled on active trials by a personal computer that displayed a virtual object, polar-projected for the current eye position. Data were also stored for use in subsequent passive trials.

In active trials, subjects performed lateral oscillatory head movements about a central point, whose perpendicular distance to the monitor was between 35 and 45 cm. In each trial three cycles were performed, with the stimulus appearing after the first half-cycle. Mean maximum displacement amplitudes about stimulus centre were $19.7 \pm 7.1°$ and $17.7 \pm 4.3°$, and mean periods were 1.9 ± 0.5 and 2.0 ± 0.5 s in experiments 1 and 2, respectively.

Stimuli were polar projections of a virtual 3D object, a partial grid of at most 10×10 square cells, each 1 cm in length, with a slant of 45° and a randomly chosen tilt. A certain number of distinct cells were randomly chosen and removed from the grid; stimuli consisted of 5, 10, 30, 60 or 100 cells in experiment 1, and of 10 cells in experiment 2. The centre of the grid was at the point on the monitor opposite the subject's initial eye position. Stimuli were drawn as one-pixel-thick white lines on a black background, with a small red fixation point at the centre.

In order to generate conflict stimuli, the initial grids, which had tilt T_p, underwent a projection from the subject's initial eye position onto a plane passing through the grid centre, with a slant of 45° but with a tilt T_m. The resulting virtual object was an irregular grid (similar to the 'Ames window' or 'Ames chair'). (In the analysis of the results, response tilts are measured with respect to T_m, with sign defined so that so that $\Delta T = T_p - T_m \geq 0$.)

Blocks of passive trials were alternated with blocks of active trials. In passive trials, subjects experienced similar optic flow as in active trials, but without head movement. Each passive trial corresponded to a preceding active trial, in that the virtual object used to generate the stimuli was identical, and that rotations of the virtual object about its centre with respect to the subject's eye were identical in passive and active trials. Let the initial eye position be $\mathbf{r_0}$ and the eye position at a given moment of an active trial be $\mathbf{r}$ (relative to the centre of the virtual object used to generate the stimulus); let $\theta = \arccos[(\mathbf{r_0} \cdot \mathbf{r})/(||\mathbf{r_0}||||\mathbf{r}||)]$ be the angle between $\mathbf{r_0}$ and $\mathbf{r}$, and let $\mathbf{a}$ be the axis generating the rotation from $\mathbf{r_0}$ to $\mathbf{r}$ (that is, $\mathbf{a}$ is parallel to $\mathbf{r_0} \times \mathbf{r}$). At the corresponding moment during the passive trial, the virtual object was rotated by angle $-\theta$ about axis $\mathbf{a}$ before being projected.

In 'twist' trials in experiment 2, the retinal optical flow underwent a 90° rotation, generated as follows. The virtual object underwent the same rotation as the eye about its centre (that is, by angle θ about axis $\mathbf{a}$). Then $\mathbf{r_0}$ was rotated by the twist angle about $\mathbf{r}$ to yield $\mathbf{r_0'}$, and a new axis $\mathbf{a'} = \mathbf{r_0'} \times \mathbf{r}$ calculated. Finally, the virtual object was rotated by angle $-\theta$ about the new axis $\mathbf{a'}$ and projected. Thus, if the twist angle were zero, the object would remain stationary (that is, in an egocentric frame it rotated about an approximately vertical axis, as in experiment 1), whereas for a 90° twist the object underwent the same rotations in the egocentric frame, but about an approximately horizontal axis.

After the disappearance of the stimulus, the projection of a virtual probe object was displayed on the monitor. The subjects' task was to align the probe—which was comprised of a circle and a perpendicular line—with the perceived plane, using a joystick.

In experiment 1, five active and five passive blocks were performed, with 100 trials in each block. In experiment 2, one active and one passive block were performed, with 160 trials per block. Eight naive volunteers participated as subjects in each of experiments 1 and 2.

1. Wallach, H. & O'Connell, D. N. The kinetic depth effect. *J. Exp. Psychol.* **45,** 205–217 (1953).
2. Braunstein, M. L. Depth perception in rotating dot patterns. *J. Exp. Psychol. Hum. Percept. Perf.* **72,** 415–420 (1962).
3. Johansson, G. Visual perception of biological motion and a model for its analysis. *Percept. Psychophys.* **14,** 210–211 (1973).
4. Ullman, S. *The Interpretation of Visual Motion* (MIT Press, Cambridge, 1979).
5. Koenderink, J. J. Optic flow. *Vision Res.* **26,** 161–179 (1986).
6. Rogers, B. & Graham, M. Motion parallax as an independent cue for depth perception. *Perception* **8,** 125–134 (1979).
7. Rogers, B. & Graham, M. Similarities between motion parallax and stereopsis in human depth perception. *Vision Res.* **22,** 261–270 (1982).
8. Rogers, S. & Rogers, B. J. Visual and nonvisual information disambiguate surfaces specified by motion parallax. *Percept. Psychophys.* **52,** 446–452 (1992).
9. Dijkstra, T. M., Cornilleau-Pérès, V., Gielen, C. C. & Droulez, J. Perception of three-dimensional shape from ego- and object-motion: comparison between small- and large-field stimuli. *Vision Res.* **35,** 453–462 (1995).
10. van Damme, W. J. & van de Grind, W. A. Non-visual information in structure-from-motion. *Vision Res.* **36,** 3119–3127 (1996).
11. Landy, M. S., Maloney, L. T., Johnston, E. B. & Young, M. Measurement and modeling of depth cue combination: in defense of weak fusion. *Vision Res.* **35,** 389–412 (1995).
12. Attneave, F. & Frost, R. The determination of perceived tridimensional orientation by minimum criteria. *Percept. Psychophys.* **6,** 391–396 (1969).
13. Longuet-Higgins, H. C. & Prazdny, K. The interpretation of a moving retinal image. *Proc. R. Soc. Lond. B* **208,** 385–397 (1980).
14. Todd, J. T. Visual information about rigid and non-rigid motion: a geometric analysis. *J. Exp. Psychol. Hum. Percept. Perf.* **8,** 238–252 (1982).
15. Wallach, H., Weisz, A. & Adams, P. A. Circles and derived figures in rotation. *Am. J. Psychol.* **69,** 48–59 (1956).
16. Adelson, E. H. Rigid objects that appear highly non-rigid. *Invest. Ophthal. Visual Sci.* **26** (Suppl.), (1985).
17. Sinha, P. & Poggio, T. Role of learning in three-dimensional form perception. *Nature* **384,** 460–463 (1996).
18. Sparrow, J. E. & Stine, W. W. The perceived rigidity of rotating eight-vertex geometric forms: extracting nonrigid structure from rigid motion. *Vision Res.* **38,** 541–556 (1998).
19. Ames, A. Visual perception and the rotating trapezoidal window. *Psychol. Monogr.* **65,** (1951).
20. Ittelson, W. H. *The Ames Demonstrations in Perception* (Princeton Univ. Press, Princeton, 1952).
21. O'Brien J. & Johnston, A. When texture takes precedence over motion in depth perception. *Perception* **29** 437–452 (2000).
22. Wade, N. J. & Hughes, P. Fooling the eyes: trompe l'oeil and reverse perspective. *Perception* **28,** 1115–1119 (1999).
23. Papathomas, T. V. See how they turn: Falso depth and motion in Hughes's reverspectives. *Proc. SPIE* **3959,** 506–517 (2000).
24. Gibson, J. J. *The Ecological Approach to Visual Perception* (Houghton-Mifflin, Boston, 1979).
25. Reinhardt-Rutland, A. H. Perceiving surface orientation: Pictorial information based on rectangularity can be overridden during observer motion. *Perception* **22,** 335–341 (1993).
26. Wallach, H. Perceiving a stable environment when one moves. *Annu. Rev. Psychol.* **38,** 1–27 (1987).
27. Ono, H. & Steinbach, M. J. Monocular steropsis with and without head movement. *Percept. Psychophys.* **48,** 179–187 (1990).
28. Snyder, L. H., Grieve, K. L., Brotchie, P. & Andersen, R. A. Separate body- and world-referenced representations of visual space in parietal cortex. *Nature* **394,** 887–891 (1998).
29. Panerai, F., Hanneton, S., Droulez, J. & Cornilleau-Pérès, V. A 6-dof device to measure head movements in active vision experiments: Geometric modeling and metric accuracy. *J. Neurosci. Meth.* **90,** 97–106 (1999).

....

Adaptive regulation of neuronal excitability by a voltage-independent potassium conductance

Stephen G. Brickley*, **Victoria Revilla**†, **Stuart G. Cull-Candy***, **William Wisden**† & **Mark Farrant***

* *Department of Pharmacology, University College London, London WC1E 6BT, UK*
† *Medical Research Council Laboratory of Molecular Biology, Medical Research Council Centre, Cambridge CB2 2QH, UK*

....

Many neurons receive a continuous, or 'tonic', synaptic input, which increases their membrane conductance, and so modifies the spatial and temporal integration of excitatory signals[1–3]. In cerebellar granule cells, although the frequency of inhibitory synaptic currents is relatively low, the spillover of synaptically released GABA (γ-aminobutyric acid)[4] gives rise to a persistent conductance mediated by the $GABA_A$ receptor[5–7] that also modifies the excitability of granule cells[8]. Here we show that this tonic conductance is absent in granule cells that lack the $\alpha 6$ and δ-subunits